J. Phys. Chem. A **2005,** *109,* 1049−1056

Gas-Phase Ion/Molecule Reactions in C_5F_8

K. Hiraoka,* K. Fujita, M. Ishida, T. Ichikawa, H. Okada, K. Hiizumi, A. Wada, and K. Takao

Clean Energy Research Center, University of Yamanashi, Takeda-4, Kofu 400-8511, Japan

S. Yamabe* and N. Tsuchida

Department of Chemistry, Nara University of Education, Takabatake-cho, Nara 630-8528, Japan

Received: March 25, 2004; In Final Form: July 8, 2004

Gas-phase ion−molecule reactions in octafluorocyclopentene (C_5F_8) were studied with a pulsed electron beam mass spectrometer. When a few Torr of major gas, CH_4, Ar, or N_2, containing ∼10 mTorr C_5F_8 was ionized by 2 keV electrons, $C_5F_8^+$, $C_5F_7^+$, $C_4F_6^+$, $C_4F_5^+$, and $C_3F_3^+$ were formed as major fragment ions. The interaction between those ions and C_5F_8 is found to be a weak electrostatic interaction. The cation$\cdots C_5F_8$ bonding energies are around 10 kcal/mol, which were reproduced well by (U)B3LYP/6-311+G(d) calculations. The proton affinity of C_5F_8 (=148.6 kcal/mol by B3LYP/6-311+G(d)) was found to be smaller than that of C_2H_4 (=162.8 kcal/mol). In the negative mode of operation, the intense signal of $C_5F_8^-$ was observed during the electron pulse. This indicates that C_5F_8 has a positive electron affinity (1.27 eV by (U)B3LYP/6-311+G(d)). The $C_5F_8^-$ ion was quickly converted to a complex $C_{10}F_{16}^-$. This complex did not react further with C_5F_8 down to 170 K. The theoretical calculation revealed that a $C_5F_7{-}F^-\cdots C_5F_8$ interaction mode in $(C_5F_8)_2^-$ was converted to a $C_5F_7^\bullet\cdots C_5F_9^-$ one via fluoride-ion transfer. The F^- ion was found to form a strong covalent bond with C_5F_8, but the interaction in $F^-(C_5F_8)$- - -C_5F_8 is a weak electrostatic interaction due to the charge dispersal in $F^-(C_5F_8)$. The halide ions except F^- interact with C_5F_8 only weakly. Thermochemical stabilities for the cluster ions $I^-(CH_3I)_n$ ($n = 1, 2$) were also determined.

Introduction

Fluorocarbon plasma is an indispensable tool for SiO_2 etching in ultra-large-scale integration (ULSI) manufacturing.[1] In the selective etching of SiO_2, fluorocarbon plasma plays a key role in preferential formation of protective fluorocarbon polymer film on Si and Si_3N_4 surfaces.[2] On the other hand, fluorocarbon film prepared by plasma-enhanced chemical vapor deposition (CVD) has attracted increasing interest as one of the most promising materials for interlayer dielectrics because of its low dielectric constant.[3] Those plasma-process technologies with fluorocarbon gases require a deeper understanding of their reactivities. In fact, the deposition mechanisms of the polymer films are still under discussion. Plasma processing gas exhausts from semiconductor fabrication cause global warming problems due to the greenhouse effect. Environmental protection requires usage of alternative fluorocarbon compounds that maintain a low global warming potential (GWP) in semiconductor processes. The atmospheric lifetimes for the conventional processing gases such as CF_4, C_2F_6, and C_4F_8 (octafluorocyclobutane) are 5×10^4, 1×10^4, and 3.2×10^3 years, respectively.[4] Therefore, the introduction of short-lived alternative gases such as C_3F_6 (<10 years)[4] and C_5F_8 (1 year)[4] to the actual manufacturing is an urgent task. The use of C_5F_8 in the CVD of fluorinated carbon films is promising for the fabrication of next-generation interlayer dielectrics, since a poly(tetrafluoroethylene)-like film with larger fluorine content and higher density can be formed.[1] Moreover, the generation of such stable molecules as CF_4 and C_2F_6 is much less in C_5F_8 plasma, which is advantageous for achieving an urgent environmental target.

While perfluorocarbons have been widely used as useful etchants for semiconductor fabrication, investigation of the ion/molecule reactions in these gases has been relatively scarce. Previously, our comprehensive studies on the negative- and positive-mode ion/molecule reactions in c-C_4F_8[5] and C_3F_6[6] were made. In the ion/molecule reactions of fluoride ion with c-C_4F_8, a covalent bond is formed in the complex $F^{-\bullet}$c-C_4F_8. In contrast, the interaction between other halide ions and c-C_4F_8 is mainly of weak electrostatic force. Theoretical calculation revealed that the halide ions interact not with the lowest unoccupied molecular orbital but with the next lowest unoccupied molecular orbital of the c-C_4F_8 molecule in the most stable cluster ions X^-(c-C_4F_8). The electron affinity of c-C_4F_8 was determined to be 12.0 ± 1.2 kcal/mol (0.52 ± 0.05 eV).[5] In the gas-phase ion−molecule reactions of hexafluoropropene (C_3F_6),[6] the positive major product ions $C_2F_4^+$, $C_3F_5^+$, and $C_3F_6^+$ were found not to form covalent bonds with the parent molecule C_3F_6. The proton affinity (PA) of C_3F_6 was found to be smaller than but close to that of C_2H_4 (experimental value, 162.8 kcal/mol;[7] the present RB3LYP/6-311+G(d)-calculated PA(C_2H_4) = 161.1 kcal/mol). The G2MP2-calculated PA(C_3F_6) is 157.26 kcal/mol. Contrary to the positive-mode ion/molecule reactions, polymerization reactions of F^-, $C_3F_5^-$, and $C_3F_6^-$ with C_3F_6 took place. The high reactivity of C_3F_6 in the negative-mode ion/molecule reactions is ascribed to the perfluoro effect.[6] The halide ions Cl^-, Br^-, and I^- were found to form cluster ions with C_3F_6.

In the present work, the positive and negative ion/molecule reactions in C_5F_8 were studied in detail. The reactivity of C_5F_8 in the negative-mode ion/molecule reactions is too high for us to measure equilibria of $C_5F_8^- + C_5F_8 \leftrightarrows C_5F_8^-(C_5F_8)$ and F^-

10.1021/jp040251k CCC: $30.25

$+ C_5F_8 \leftrightarrows C_5F_9^-$. Interactions between C_5F_8 and fragment cations are weak and of about 10 kcal/mol binding energies. The $-CF_2-CF_2-$ moiety of C_5F_8 is linked with those cations weakly. Particular interest lies in the decomposition pattern of the cyclopentene ring to afford small fragment cations. Rupture of the five-membered ring and the subsequent formation of fragment cations were investigated theoretically.

Experimental and Theoretical Methods

The experiments were made with a pulsed electron beam high-pressure mass spectrometer.[8,9] The major gas, CH_4, Ar, or N_2, at a few Torr was purified by passing it through a dry ice acetone cooled 5A molecular sieve trap. The reagent gases, C_5F_8 and halide-ion forming gases (NF_3 for F^-, CCl_4 for Cl^-, CH_2Br_2 for Br^-, and CH_3I for I^-), were introduced into the major gas through stainless steel capillaries (1 m long × 0.1 mm inner diameter). The sample gas was ionized by a pulsed 2 keV electron beam. The ions produced in the field-free ion source were sampled through a slit made of razor blades and were mass analyzed by a quadrupole mass spectrometer (ULVAC, MSQ-400, $m/z = 1-550$). The width and the length of the slit were 10 μm and 1 mm, respectively. Since the width of the slit was smaller than the mean free path of a few Torr sample gas, the ions were sampled through the slit by the molecular flow; i.e., the adiabatic cooling of the effusing gas during the ion sampling was negligible.

Geometries of C_5F_8, its fragment ions, and ion$\cdots C_5F_8$ complexes were optimized by (U)B3LYP/6-311+G(d)[10] calculations. Isomeric geometries were carefully examined. The geometries that are less stable than those in Figures 3−5 are in the Supporting Information. The subsequent vibrational analyses were made to check whether those geometries are correctly at the energy minima and to obtain zero-point vibrational energies (ZPEs). Proton and electron affinities and binding energies (ΔE's) were evaluated by the (U)B3LYP/6-311+G(d) electronic energies and ZPEs. All the calculations were performed by the use of the Gaussian 98 program[11] installed at the Compaq ES40 computer in the Information Processing Center (Nara University of Education).

Results and Discussion

Positive-Mode Ion/Molecule Reactions. The ions $C_5F_8^+$, $C_5F_7^+$, $C_4F_6^+$,$C_4F_5^+$, $C_5F_6^+$, and $C_3F_3^+$ were formed when the major gas of a few Torr N_2 or Ar containing ∼10 mTorr of C_5F_8 was ionized by a 2 keV electron pulse. The order of the ion intensities is $C_5F_8^+ \geq C_5F_7^+ \approx C_4F_6^+ \gg C_4F_5^+ > C_5F_6^+ > C_3F_3^+$. These ions did not react further with C_5F_8 at room temperature and above. With decrease of the ion source temperature, cations associated with C_5F_8 were formed.

$$C_5F_8^+ + C_5F_8 = C_5F_8^+(C_5F_8) \qquad (1)$$

$$C_5F_7^+ + C_5F_8 = C_5F_7^+(C_5F_8) \qquad (2)$$

$$C_4F_6^+ + C_5F_8 = C_4F_6^+(C_5F_8) \qquad (3)$$

$$C_4F_5^+ + C_5F_8 = C_4F_5^+(C_5F_8) \qquad (4)$$

$$C_3F_3^+ + C_5F_8 = C_3F_3^+(C_5F_8) \qquad (5)$$

The measurements of the thermochemical data for clustering reactions 1−5 were made as described below.

$C_5F_8^+$. The $C_5F_8^+$ ion observed in a few Torr of N_2 major gas containing ∼10 mTorr C_5F_8 was mainly formed by charge-transfer reaction 6 or 8.

$$N_2^+ + C_5F_8 \rightarrow N_2 + C_5F_8^+ \qquad (6)$$

$$N_2^+ + N_2 + N_2 \rightarrow N_4^+ + N_2 \qquad (7)$$

$$N_4^+ + C_5F_8 \rightarrow 2N_2 + C_5F_8^+ \qquad (8)$$

Since the experimental ionization potential (IP) of C_5F_8 is not available (the present calculated IP value is 11.2 eV (257.8 kcal/mol)), the enthalpy changes for reactions 6 and 8 were estimated by the (U)B3LYP/6-311+G(d) calculated values. They are −108.0 and −67.8 kcal/mol, respectively. Because the exothermic energy in the charge-transfer reaction is generally imparted to the newly formed ions, a highly excited $C_5F_8^+$ may be formed by reaction 6 or 8. Thus the ring rupture of the product ion $C_5F_8^+$ may be conceivable.

The associated ion $C_5F_8^+(C_5F_8)$ started to be formed when the ion source temperature was decreased below 280 K under the present experimental conditions. However, the equilibrium between $C_5F_8^+$ and $C_5F_8^+(C_5F_8)$ was not observed even a few milliseconds after the electron pulse, i.e., slow growth of $C_5F_8^+(C_5F_8)$ at the expense of $C_5F_8^+$. The slow conversion of $C_5F_8^+$ to $C_5F_8^+(C_5F_8)$ suggests either that the rate of the clustering reaction is slow due to the steric hindrance (i.e., an entropy barrier) for the formation of the cluster ion or that the reaction of $C_5F_8^+$ with C_5F_8 to form $C_5F_8^+(C_5F_8)$ is irreversible. The complex $C_5F_8^+(C_5F_8)$ may not have a strong covalent bond because $C_5F_8^+(C_5F_8)$ was observed only at lower temperature ($\leq$ ∼280 K). We may conclude that the complex $C_5F_8^+(C_5F_8)$ is only a cluster ion. The relative intensity of $C_5F_8^+(C_5F_8)$ to $C_5F_8^+$ increased gradually with decrease of the ion source temperature, but the equilibrium between them could not be established down to ∼220 K. Interestingly, however, equilibria between $C_5F_8^+$ and $C_5F_8^+(C_5F_8)$ started to be observed even right after the electron pulse below 220 K. A very similar trend was observed in the clustering reaction of $C_3F_6^+$ with C_3F_6.[6] The quick establishment of equilibrium below 220 K suggests that the entropically more favored (less steric hindrance) "isomeric" cluster ion $C_5F_8^+(C_5F_8)$ is formed below 220 K.

There might be another possibility that the $C_5F_8^+$ ion in the cluster $C_5F_8^+(C_5F_8)$ observed above 220 K maintains the intact ring structure; i.e., the ring $C_5F_8^+$ forms a stronger bond than the ring-opened one. To obtain more information on the structure of $C_5F_8^+$, the equilibrium constants for reaction 1 were measured using a few Torr of helium as a major gas. From the recombination energy 24.59 eV of He^+, the exothermicity for reaction 9 may be estimated to be ∼14.5 eV.

$$He^+ + C_5F_8 \rightarrow He + C_5F_8^+ \qquad (9)$$

This high exothermicity is likely to lead to the ring rupture of the product ion $C_5F_8^+$. In Figure 1, the van't Hoff plots obtained using N_2 (open circles) are plotted together with those obtained using He (filled circles). Both van't Hoff plots lie on the same straight line. This finding suggests that all the product ion $C_5F_8^+$ formed by reactions 6, 8, and 9 undergoes the ring rupture to give the open-chain cation radical. However, we have no idea to what extent the ring-opened $C_5F_8^+$ is contaminated by the ring-closed $C_5F_8^+$. The thermochemical data obtained from the van't Hoff plots in Figure 1 are summarized in Table 1. The

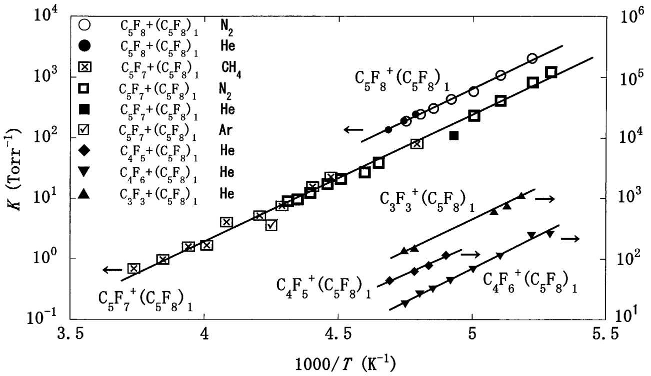

Figure 1. van't Hoff plots for clustering reactions of $C_5F_8^+$, $C_5F_7^+$, $C_4F_6^+$, $C_4F_5^+$, and $C_3F_3^+$ with C_5F_8. The carrier gas used is shown in the inset.

measurement of the equilibria for reaction 1 was also made using a few Torr of Ar gas as a major gas. However, the observed ion intensities became increasingly weak at lower temperatures due to charging of the ion source and reliable equilibrium constants could not be obtained.

Ring-rupture reactions and fragmentations of positive ions were investigated computationally.

Scheme 1 shows four routes, routes i−iv. In route i, the fluorine atom of $C_5F_8^+$ is taken off to give **5** ($C_5F_7^+$). An allyl-cation moiety is involved in **5**. In route ii, ring rupture of **1** and the subsequent CF_2 elimination take place. A diene cation radical **4** ($C_4F_6^+$) is generated. The detailed reaction paths are shown in Figure 2a. In route iii, the linear-diene cation radical **4** isomerizes to a cyclobutene cation radical **6**. This radical may evolve the F atom readily to give **7** ($C_4F_5^+$) with the allyl-cation moiety (Scheme 2). In route iv, an F atom migrates to afford an intermediate **8**. The cation radical **8** undergoes an intramolecular shift of the CF_3 group. During the shift, the group may be pushed away, which leads to a cyclopropyl cation **9** ($C_3F_3^+$). The detailed paths of route iv are exhibited in Figure 2b. Figure 2a shows reaction paths of the ring opening and one fragmentation of $C_5F_8^+$ in route ii of Scheme 1. ΔE of TS(**1**→**2**) = 15.43 kcal/mol (TS, transition state) is a calculated activation energy and is much smaller than the exothermic energies (108.0 and 67.8 kcal/mol) evolved in reactions 6 and 8. Thus, the ring-opening route is quite an energetically accessible process. The resultant open-chain intermediate **2** may undergo C−C bond cleavage. A representative fragmentation path is also shown in Figure 2a. The CF_2 elimination TS, TS(**2**→**3**), has $\Delta E = +23.89$ kcal/mol, which may also be overcome by the large exothermicities in reactions 6 and 8. Figure 2b shows the reaction path of route iv of Scheme 1. The diene cation radical **4** is isomerized to **8** via the fluorine-shift TS, TS(**4**→**8**). The cation radical **8** has a CF_3 group. The group may migrate via TS(**8**→**8**). The TS has a geometry of $C_3F_3^+$ and CF_3. During the migration, the CF_3 group happens to be pushed away by the centrifugal force. A cyclopropyl cation **9** ($C_3F_3^+$) is afforded.

TABLE 1: Thermochemical Data for Gas-Phase Clustering Reactions

	$-\Delta H°$ (kcal/mol)	$-\Delta S°$ (cal/mol·K)
$C_5F_8^+ + C_5F_8 = C_5F_8^+(C_5F_8)$	10.3 ± 0.3	25 ± 4
$C_5F_7^+ + C_5F_8 = C_5F_7^+(C_5F_8)$	9.4 ± 0.2	24 ± 3
$C_4F_6^+ + C_5F_8 = C_4F_6^+(C_5F_8)$	9.6 ± 0.3	27 ± 3
$C_4F_5^+ + C_5F_8 = C_4F_5^+(C_5F_8)$	9.2 ± 0.4	23 ± 5
$C_3F_3^+ + C_5F_8 = C_3F_3^+(C_5F_8)$	9.3 ± 0.3	22 ± 4
$F^- + C_5F_8 = F^-(C_5F_8)$	≥30	
$F^-(C_5F_8) + C_5F_8 = F^-(C_5F_8)_2$	6.7 ± 0.3	19 ± 3
$Cl^- + C_5F_8 = Cl^-(C_5F_8)$	13.8 ± 0.2	19 ± 3
$Cl^-(C_5F_8) + C_5F_8 = Cl^-(C_5F_8)_2$	11.0 ± 0.2	22 ± 3
$Br^- + C_5F_8 = Br^-(C_5F_8)$	12.7 ± 0.3	19 ± 4
$I^- + C_5F_8 = I^-(C_5F_8)$	10.0 ± 0.2	20 ± 3
$I^- + CH_3I = I^-(CH_3I)$	7.8 ± 0.2 9.0[a]	17 ± 3 16.4[a]
$I^-(CH_3I) + CH_3I = I^-(CH_3I)_2$	7.0 ± 0.2	20 ± 3

[a] Reference 13.

Geometries of the $C_5F_8(C_5F_8)^+$ complex were examined. Since the energetically accessible ring rupture of $C_5F_8^+$ has been suggested, its complex needs to be investigated. Figure 3 shows the obtained two geometries. The electrophilic centers of $C_5F_8^+$ are the vinyl carbon atoms in part a and the allyl ones in part b, respectively. The nucleophilic centers of C_5F_8 are fluorine atoms on sp^3 carbon atoms. Isomer a is much more stable with the binding energy of 14.66 kcal/mol, which is somewhat larger than the present experimental value, $-\Delta H° = 10.3 \pm 0.3$ kcal/

SCHEME 1: Fragmentation Routes Affording Cation Species[a]

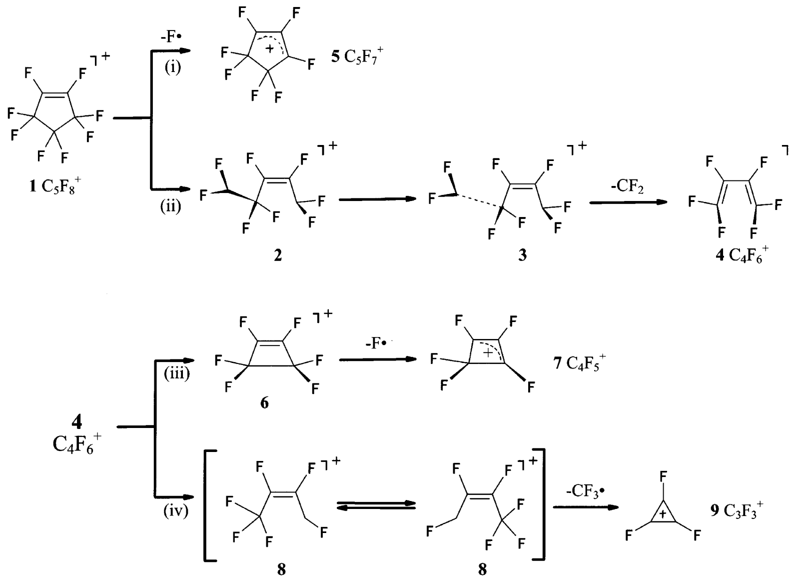

[a] The fluorine-evolving paths, **1**→**5** and **6**→**7**, lead to ring products, **5** and **7**, respectively, with allyl-cation moieties. Route ii, **1**→**2**→**3**→**4**, is shown in Figure 2a. Route iv, **4**→**8**→**8**, is shown in Figure 2b.

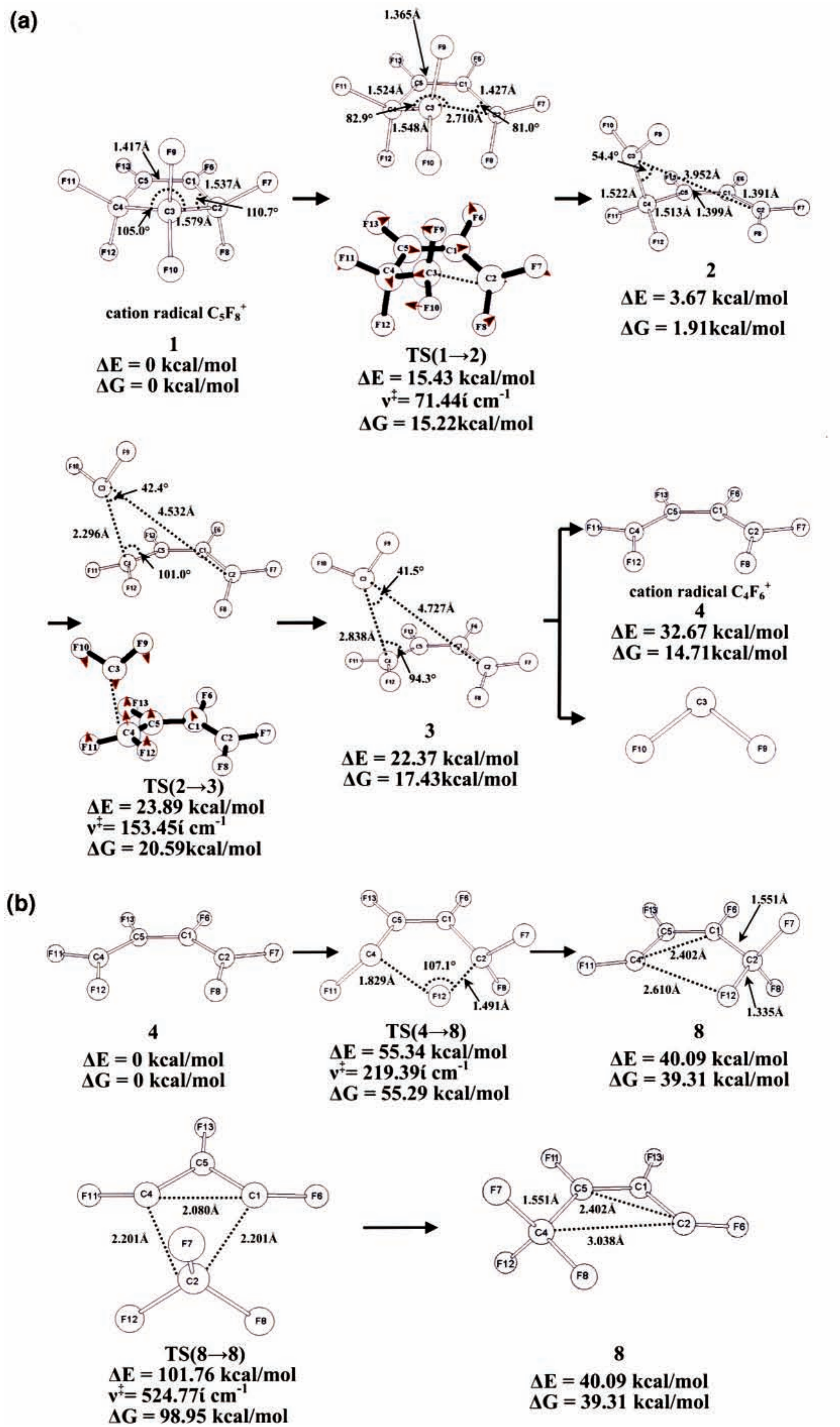

Figure 2. (a) Reaction paths of the ring opening and the subsequent CF_2 elimination of $C_5F_8^+$. ΔE is the energy difference relative to that of **1**, $C_5F_8^+$. $\Delta G(T = 300\text{ K}, P = 1\text{ atm})$ is the difference of Gibbs free energies. TS stands for transition state, where reaction-coordinate vectors corresponding to the sole imaginary frequencies ($\nu^{\ddagger}$s) are exhibited. (b) Reaction paths of the isomerization in route iv of Scheme 1.

SCHEME 2 An Allyl Cation Moiety Which Stabilizes Fragment Species

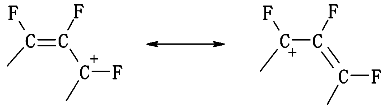

mol in Table 1. The vinyl site of $C_5F_8^+$ may be linked more strongly to C_5F_8 than the allyl one.

$C_5F_7^+$. When a few Torr of CH_4 containing ~10 mTorr of C_5F_8 was ionized by 2 keV electrons, positive ions in the order of $C_5F_7^+ \geq C_2H_5^+ \gg C_5F_8^+ \approx C_4F_6^+$ were formed. The major ions formed from CH_4 by electron impact are CH_4^+ and CH_3^+. These ions react with CH_4 with collision rates to form CH_5^+ and $C_2H_5^+$, respectively. It was found that CH_5^+ reacts with C_5F_8 nearly with a collision rate to form $C_5F_7^+$.

$$CH_5^+ + C_5F_8 \rightarrow [C_5F_8H^+]^* + CH_4 \rightarrow C_5F_7^+ + HF + CH_4 \quad (10)$$

If the proton-transfer reaction $[CH_5^+ + C_5F_8 \rightarrow [C_5F_8H^+]^* + CH_4]$ has some energy barrier or is endothermic, reaction 10 would not occur with collision rate. The collision rate for reaction 10 indicates that the reaction is exothermic, i.e., the PA of C_5F_8 is larger than that of CH_4 (124.5 kcal/mol[7]) and the protonated $H^+C_5F_8$ dissociates unimolecularly to $C_5F_7^+$ and HF. In contrast, $C_2H_5^+$ was converted slowly to $C_5F_7^+$ by reaction 11.

$$C_2H_5^+ + C_5F_8 \rightarrow C_2H_4 + C_5F_7^+ + HF \quad (11)$$

This suggests that reaction 11 is endothermic or at least has some energy barrier; i.e., PA(C_5F_8) may be smaller than PA(C_2H_4) (162.8 kcal/mol[7]).

The equilibria for reaction 2 were established right after the electron pulse. This means that there is no entropy barrier for the formation of the most stable cluster ion $C_5F_7^+(C_5F_8)$. The van't Hoff plots for reaction 2 using CH_4, N_2, Ar, and He as major gases are displayed in Figure 1. All the equilibrium constants obtained for these major gases fall in the same straight line within the experimental error. This finding suggests that $C_5F_7^+$ suffers from ring rupture during the ion formation for all major gases of CH_4, Ar, N_2, and He. Thermochemical data for reaction 2 are shown in Table 1.

Figure 4a−c shows three isomers of $H^+C_5F_8$. Species a and b are composed of $C_5F_7^+$ and hydrogen fluoride. Isomer a is 24.77 and 22.57 kcal/mol more stable than isomers b and c, respectively. In isomer a, the allyl-cation skeleton is attained for stabilization. The RB3LYP/6-311+G(d) ZPE proton affinity of C_5F_8 is 148.56 kcal/mol. Figure 4d shows a geometry of $C_5F_7^+(C_5F_8)$ where the allyl-cation moiety of $C_5F_7^+$ is linked with two fluorine atoms (F8 and F10) of C_5F_8. The binding energy ($-\Delta E$) is computed to be 8.03 kcal/mol, which is in good agreement with the present experimental data, $-\Delta H° = 9.4 \pm 0.3$ kcal/mol.

$C_4F_6^+$, $C_4F_5^+$, and $C_3F_3^+$. The measurements of the equilibria for reactions 3−5 were performed using a few Torr of He as a major gas. The order of the intensities of observed ions is $C_3F_3^+ \geq C_5F_7^+ > C_5F_8^+ \approx C_4F_6^+ \approx C_4F_5^+ \approx C_4F_4^+ \gg C_5F_6^+ \approx C_3F_4^+ \approx C_2F_4^+$. As in the case of $C_5F_7^+$, the equilibria for reactions 3−5 were established almost right after the electron pulse. This indicates that the formation of most stable cluster ions do not have any appreciable entropy barrier in the reaction coordinates as in the case of reaction 2. The van't Hoff plots for reactions 3−5 are displayed in Figure 1, and thermochemical data obtained from the van't Hoff plots are summarized in Table 1. In the table, enthalpy changes ($-\Delta H°$) for reactions 1−5 are of the same order. The rather small enthalpy changes ($\leq$ ~10 kcal/mol) for these reactions suggest that the five cations $C_5F_8^+$, $C_5F_7^+$, $C_4F_6^+$, $C_4F_5^+$, and $C_3F_3^+$ are coordinated to C_5F_8 weakly and similarly.

Figure 5 shows geometries of $C_4F_6^+(C_5F_8)$, $C_4F_5^+(C_5F_8)$, and $C_3F_3^+(C_5F_8)$. The fragment ion $C_4F_6^+$ has been generated as **4** in Figure 2a. A ring isomer **6** (cyclobutene) of $C_4F_6^+$ in Figure 5a is present, which is however 36.5 kcal/mol less stable than **4** and is converted with the accessible energy change to **7** ($C_4F_5^+$) and $F^\bullet$. A weak and long-range (~3 Å) bond complex of $C_4F_6^+(C_5F_8)$ is obtained. The calculated binding energy, $-\Delta E = 7.51$ kcal/mol, is somewhat smaller than the observed one, $-\Delta H° = 9.6 \pm 0.3$ kcal/mol in Table 1. In Figure 5b, the fragment ion $C_4F_5^+$ is found to have uniquely a four-membered ring with with C_{2V} symmetry. The $C_4F_5^+(C_5F_8)$ complex is calculated to have a binding energy $-\Delta E = 7.78$ kcal/mol, which is comparable with the observed one, $-\Delta H° = 9.2 \pm 0.4$ kcal/mol. In Figure 5c, a geometry of the fragment ion $C_3F_3^+$ associated with C_5F_8 is shown. The $-\Delta E$ value is 7.65 kcal/mol, which is also comparable to the experimental one, $-\Delta H° = 9.3 \pm 0.3$ kcal/mol.

Negative-Mode Ion/Molecule Reactions. *$C_5F_8^-(C_5F_8)_n$*. In the negative mode of operation, a very strong $C_5F_8^-$ was formed as a major ion during the electron pulse for a few Torr of major gas (CH_4, N_2, or Ar) containing ~10 mTorr of C_5F_8. The rapid electron capture by the C_5F_8 molecule clearly indicates that the electron affinity of C_5F_8 is positive in agreement with the results reported by Pai et al.[12] The primary $C_5F_8^-$ ion was found to decay rapidly right after the electron pulse and was completely

$C_5F_8 \ldots C_5F_8^+$

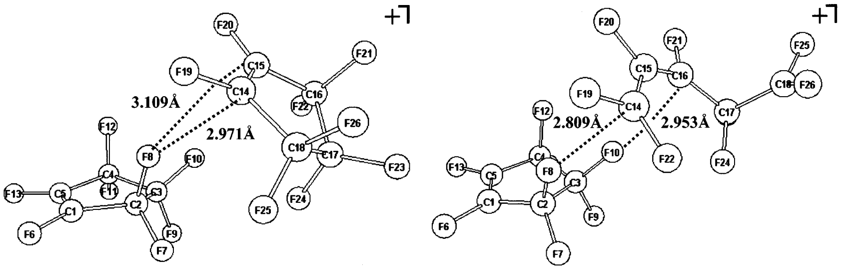

(a)
$C_5F_8^+ \ldots C_5F_8$
-ΔE= 14.66 kcal/mol

(b)
$C_5F_8^+$(open)$\ldots C_5F_8$
-ΔE=6.37 kcal/mol

Figure 3. Two isomers of $C_5F_8^+(C_5F_8)$. ΔE is a stabilizing energy, which is comparable to $-\Delta H°$ (Table 1). In isomer b, the right-side moiety is the ring-opened cation radical which is shown as **2** in Figure 2. Isomer a with $\Delta E = -14.66$ kcal/mol is much more stable than isomer b with $\Delta E = -6.37$ kcal/mol.

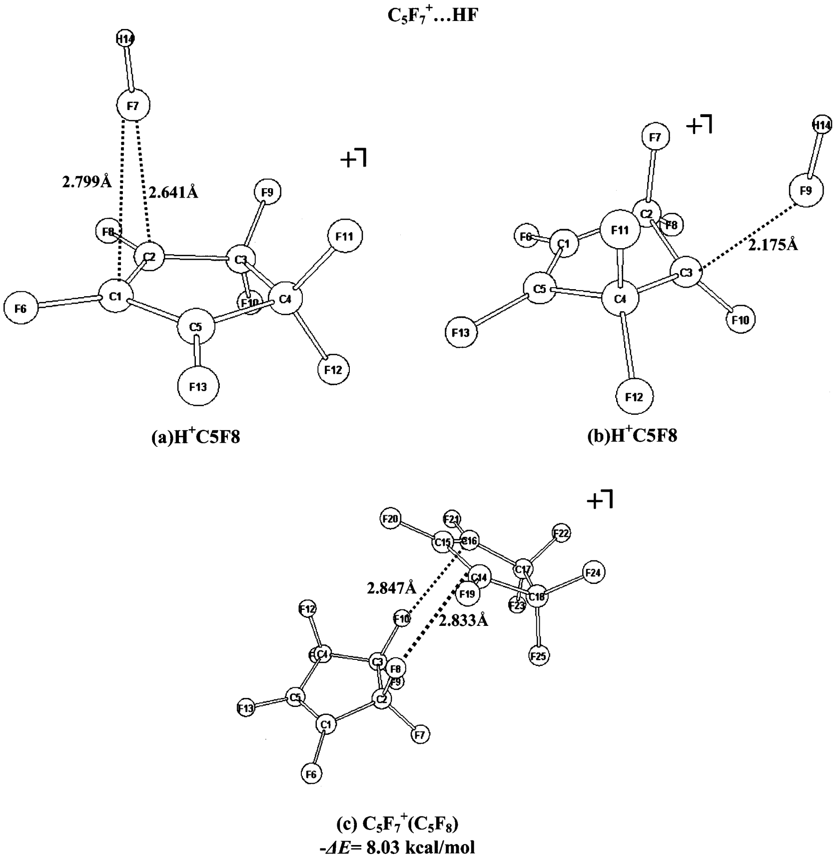

(a)H^+C5F8 (b)H^+C5F8

(c) $C_5F_7^+(C_5F_8)$
$-\Delta E$= 8.03 kcal/mol

Figure 4. Geometries of the protonated C_5F_8 (a,b) and $C_5F_7^+(C_5F_8)$ (c).

converted to the "dimer" anion $C_{10}F_{16}^-$ (95%) and also to $C_5F_9^-$ (5%) at ~300 K. This might indicate the occurrence of clustering reaction 12 as well as the unimolecular decomposition of the intermediate complex $[C_5F_8^-(C_5F_8)]^*$ to form $F^-(C_5F_8)$ and C_5F_7 in reaction 13.

$$C_5F_8^- + C_5F_8 \rightleftarrows C_5F_8^-(C_5F_8) \qquad (12)$$

$$C_5F_8^- + C_5F_8 \rightleftarrows [C_5F_8^-\cdots C_5F_8]^* \rightarrow [C_5F_7\cdots C_5F_9^-]^* \rightarrow F^-(C_5F_8) + C_5F_7 \qquad (13)$$

$$\rightarrow [C_5F_7\cdots C_5F_9^-]^* + M \rightarrow C_5F_9^-(C_5F_7) \qquad (14)$$

Although the ion source temperature was increased up to 650 K, the dimer anion did not dissociate to give the monomer $C_5F_8^-$. That is, the equilibrium for reaction 12 was not observed. The experiment above 650 K was not possible due to the serious charging of the ion source.

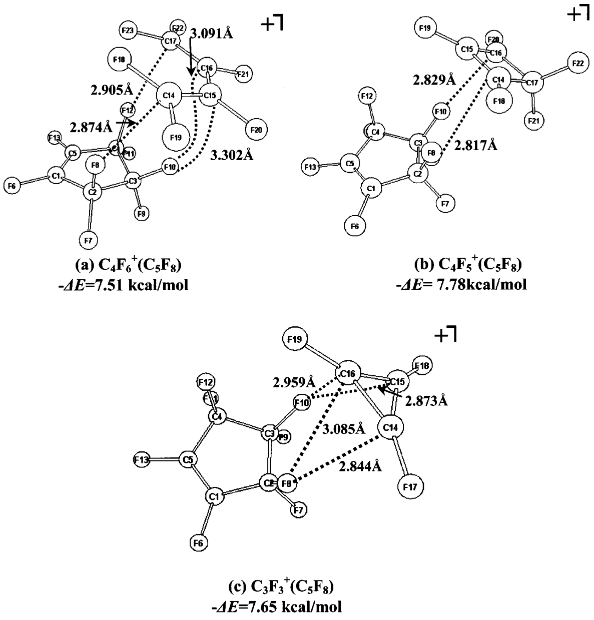

(a) $C_4F_6^+(C_5F_8)$
$-\Delta E$=7.51 kcal/mol

(b) $C_4F_5^+(C_5F_8)$
$-\Delta E$= 7.78kcal/mol

(c) $C_3F_3^+(C_5F_8)$
$-\Delta E$=7.65 kcal/mol

Figure 5. Geometries of $C_4F_6^+(C_5F_8)$, $C_4F_5^+(C_5F_8)$, and $C_3F_3^+(C_5F_8)$.

To obtain more detailed information on the structure of the associated ions, theoretical calculation was made on $C_{10}F_{16}^-$. Figure 6 exhibits geometries of $C_5F_8^-(C_5F_8)$. The anomalous appearance of the dimer might be related to formation of new C−C bonds. A cycloadduct dimer is obtained in part a, which is however an unstable species ($\Delta E = +3.33$ kcal/mol). Another isomer of $C_5F_8^-(C_5F_8)$ was sought. A weakly interacting system was obtained and is shown at the left of Figure 6b. An F−C bond (F14−C15) is linked to the vinyl bond (C1−C5) with C1···F14 and C5···F14 distances of ~3 Å. The long-range coordination gives a binding energy $-\Delta E = 5.68$ kcal/mol. The $C_5F_8\cdots C_5F_8^-$ species was found to undergo a fluoride-ion shift reaction (reaction 13) with a very small activation energy, $-\Delta E = 1.64$ kcal/mol. The resultant $C_5F_9^-(C_5F_7)$ complex is 3.61 kcal/mol more stable than $C_5F_8^-(C_5F_8)$. Thus, the $C_5F_8^-(C_5F_8)$ dimer is only transient and is rapidly converted to $C_5F_9^-(C_5F_7)$. The calculated weak bond of $C_5F_8^-(C_5F_8)$ and the feasibility of its isomerization indicate that the complex $C_{10}F_{16}^-$ has the structure not of $C_5F_8^-(C_5F_8)$ but of $C_5F_9^-(C_5F_7)$.

With increase in the ion source temperature, the ratio of the ion intensities $I[C_5F_9^-]/I[C_{10}F_{16}^-]$ was found to increase. This indicates that the branching ratio of reaction 13 to reaction 14 increases with temperature. This is reasonable because the

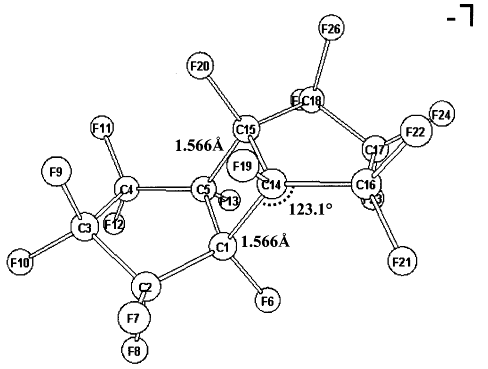

(a)
-*ΔE*= -3.33 kcal/mol (unstable)

(b)

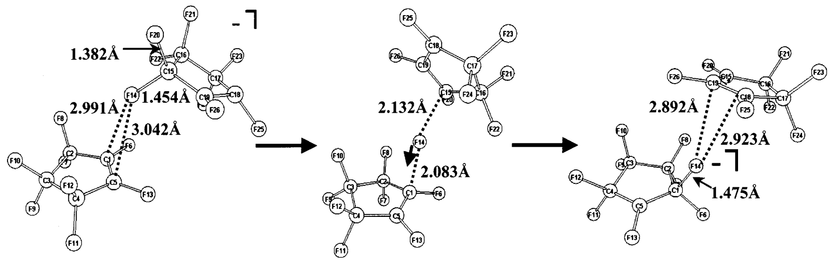

$C_5F_8...C_5F_8^-$
ΔE=0 kcal/mol

TS
ΔE=1.64 kcal/mol
$v^{‡}$=74.83*i* cm^{-1}

$C_5F_9^-...C_5F_7•$
ΔE= -3.61 kcal/mol

-*ΔE*=5.68 kcal/mol

Figure 6. Geometries of $C_5F_8^-(C_5F_8)$. In part a, a symmetric dimer involving the cyclobutane moiety is shown, which is however less stable than the separated state of C_5F_8 and $C_5F_8^-$. In part b, a reaction path of the F^- migration is shown. TS is a transition state. ΔE's are relative energies, and ΔE is a binding energy. Since C_5F_8 has an electron deficient cyclopentene ring, the one-electron supply strengthens the ring. In fact, the distances of four C−C single bonds in $C_5F_8^-$ are smaller than those in C_5F_8. The ring-opened isomer of $C_5F_8^-$ is unlikely.

lifetime of the intermediate complex $[C_5F_9^-\cdots C_5F_7]^*$ decreases with increase of temperature and the collisional stabilization (reaction 14) becomes increasingly less efficient at higher temperature.

With the ion source temperature above ~600 K, strong growths of newly formed ions such as F_2^-, $C_2F_2^-$, and $C_2F_3^-$ in addition to the persistent appearance of $C_5F_9^-$ are observed at the expense of $C_5F_9^-(C_5F_7)$. At present, we do not understand the reaction mechanisms for the formation of those ions.

It was found that the complex $C_5F_9^-(C_5F_7)$ stayed as a strongest ion down to the ion source temperature of ~162 K (just above the condensation point of ~10 mTorr C_5F_8). This means that the conversion of the complex $C_5F_9^-(C_5F_7)$ to the cluster ion $C_5F_9^-(C_5F_7)\cdots(C_5F_8)$ is minor or even negligible in the lower temperature region. Because the mass range of the quadrupole mass spectrometer used in this work is limited in the range of $m/z = 1-550$, $C_5F_9^-(C_5F_7)\cdots(C_5F_8)$ (m/z 636) could not be measured. In the complex $C_5F_9^-(C_5F_7)$, the anion center is the C5 atom in the $C_5F_9^-$ moiety. The carbanion is near F substituents and cannot be coordinated to the vinyl carbon atoms of the second C_5F_8 (exchange repulsive interference against the coordination). The negative charges in $C_5F_9^-(C_5F_7)$ are so localized in the carbanion that the interaction between $C_5F_9^-(C_5F_7)$ and the second C_5F_8 ligand may be very weak.

$X^-(C_5F_8)_n$ (X = F, Cl, Br, and I). The thermochemical stabilities of the cluster ions of halide ions (X^-) with C_5F_8 were studied by observing the equilibria for clustering reaction 15.

$$X^-(C_5F_8)_{n-1} + C_5F_8 = X^-(C_5F_8)_n \qquad (15)$$

Figure 7 shows the van't Hoff plots for reaction 15 for X = F, Cl, Br, and I. The thermochemical data obtained are summarized in Table 1.

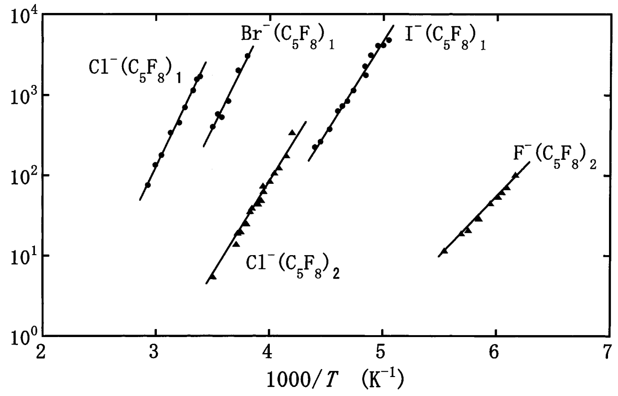

Figure 7. van't Hoff plots for clustering reactions $X^-(C_5F_8)_{n-1} + C_5F_8 = X^-(C_5F_8)_{n-1}$, X = F, Cl, Br, and I.

In reaction 15 for X = F, the F^- ion decayed rapidly and is totally converted to $F^-(C_5F_8)$ after the electron pulse. The equilibrium for reaction 15 with $n = 1$ for X = F could not be established with the ion source temperature up to 650 K; i.e., $F^-(C_5F_8)$ does not dissociate into F^- and C_5F_8 up to 650 K (measurement above 650 K could not be made due to charging of the ion source). Since the experimental equilibrium constant K (=$[C_5F_9^-]/[F^-][C_5F_8]$) at 650 K is estimated to be larger than 100 Torr^{-1}, the enthalpy change $-\Delta H°$ for reaction $[F^- + C_5F_8 \leftrightarrows F^-C_5F_8]$ can be roughly estimated to be >35 kcal/mol from the van't Hoff equation, $-\Delta G° = RT \ln K = -\Delta H° + T\Delta S°$. Here, the entropy change $-\Delta S°$ is assumed to be 25−30 cal/mol·K. This suggests that the bond energy of $F^-\cdots C_5F_8$ is larger

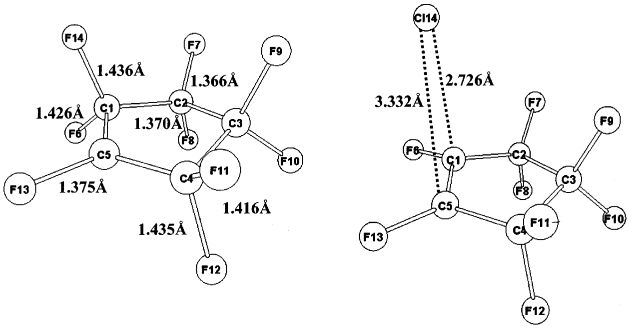

$F^-(C_5F_8)$
$-\Delta E = 47.72$ kcal/mol

$Cl^-(C_5F_8)$
$-\Delta E = 12.98$ kcal/mol

Figure 8. Geometries of $X^-(C_5F_8)$, X = F and Cl. For X = Cl, (RB3LYP/6-311+G(2d)), [RB3LYP/6-311+G(2df,p)], and {RB3LYP/6-311+G(3df,p)} data are also shown.

than ~35 kcal/mol, i.e., covalent bond formation in the complex. The dimer anion $F^-(C_5F_8)_2$ started to be formed at about room temperature. However, equilibria between $F^-(C_5F_8)$ and $F^-(C_5F_8)_2$ could not be observed down to ~180 K due to the slow growth of $F^-(C_5F_8)_2$ at the expense of $F^-(C_5F_8)$. There seems to be some entropy barrier for the formation of the most stable $F^-(C_5F_8)_2$ as in the case of reaction 1 with $n = 1$. It was found that sound equilibria between $F^-(C_5F_8)$ and $F^-(C_5F_8)_2$ were observed below ~180 K down to 162 K (just above the condensation point of the reagent gas C_5F_8). The cluster ion $F^-(C_5F_8)_2$ observed in the temperature range of 180−162 K may have a different structure from that observed in the higher temperature region, i.e., the entropically favored structure. The weak bond of the dimer anion $F^-(C_5F_8)\cdots C_5F_8$ (6.7 ± 0.3 kcal/mol) indicates that the negative charge is well delocalized in $F^-(C_5F_8)$ (i.e., charge transfer $F^- \rightarrow C_5F_8$) and the nature of bonding changes drastically from covalent to electrostatic with $n = 1 \rightarrow 2$.

The enthalpy changes for reactions 15 for X = Cl, Br, and I are of the electrostatic interaction (Table 1). Without the capability of the covalent bond formation, the weak electrostatic interaction is preferred for $X^-(C_5F_8)$ with X = Cl, Br, and I. In general, the C_5F_8 molecule shows a larger reactivity in the negative-mode ion/molecule reactions than in the positive-mode ones. This character comes from the perfluoro effect.[6]

Figure 8 shows geometries of $X^-(C_5F_8)$, X = F and Cl. In $F^-(C_5F_8)$, the fluoride ion is captured as a substituent, and the cluster has C2 symmetry. A large binding energy, $-\Delta E = 47.72$ kcal/mol, is obtained. This value is too large for us to measure the equilibrium in reaction 15 with $n = 1$ and X = F. In contrast to $F^-(C_5F_8)$, the chloride ion is bound weakly to C_5F_8. The difference of two C$\cdots$Cl distances (2.726 and 3.332 Å in Figure 8) indicates a slight charge transfer, $Cl^- \rightarrow \Pi^*(C{=}C)$. The calculated binding energy, $-\Delta E = 12.98$ kcal/mol, is in good agreement with the observed one, $-\Delta H° = 13.8 \pm 0.2$ kcal/mol, in Table 1. Basis set dependence of the binding energies was assessed by the use of 6-311+G(2d), 6-311+G(2df,p), and 6-311+G(3df,p) as well as 6-311+G(d). The four basis sets give 12−13 kcal/mol energies and similar C$\cdots$Cl distances. The almost invariant calculated values indicate that the RB3LYP/6-311+G(d) method is of acceptable quality for the present clusters.

In the present experiment, equilibria for reaction 16 ($n = 1$, 2) were also measured using a few Torr of methane containing 3−10 mTorr of CH_3I (van't Hoff plots not shown).

$$I^-(CH_3I)_{n-1} + CH_3I = I^-(CH_3I)_n \qquad (16)$$

The rather small values of $-\Delta H°_{0,1}$ (7.8 ± 0.2 kcal/mol) and $-\Delta H°_{1,2}$ (7.0 ± 0.2 kcal/mol) indicate that the interactions in the cluster ions are of electrostatic nature. The close values of $-\Delta H°_{n-1,n}$ with $n = 1$ and 2 suggests that two CH_3I ligands interact with the core ion I^- symmetrically with the sandwich $D_{\infty h}$ geometry, ICH_3- - -I^-- - -H_3CI.

Concluding Remarks

Gas-phase clustering reactions of C_5F_8 and its fragment ions have been investigated experimentally and computationally. In cation clusters $C_5F_8^+(C_5F_8)$, $C_5F_7^+(C_5F_8)$, $C_4F_6^+(C_5F_8)$, $C_4F_5^+(C_5F_8)$, and $C_3F_3^+(C_5F_8)$, the binding energies are about 10 kcal/mol or less. Fragment cations interact not with the vinyl moiety of C_5F_8 but with fluorine substituents on the sp^3 carbon atoms with intermolecular distances of ~3 Å. In anion clusters, thermochemical data of $X^-(C_5F_8)_n$ were obtained successfully except for $F^-(C_5F_8)$. The measured binding energies are in fair agreement with the computed ones.

Acknowledgment. The authors thank the Zeon Corporation for supplying C_5F_8 gas.

Supporting Information Available: Figures S1−S3 which exhibit geometries other than those shown in Figures 3b, 4d, and 5c. This material is available free of charge via the Internet at http://pubs.acs.org.

References and Notes

(1) Takahashi, K.; Itoh, A.; Nakamura, T.; Tachibana, K. *Thin Solid Films* **2000**, *374*, 303.

(2) Schaepkens, M.; Standaert, T. E. F. M.; Rueger, N. R.; Sebel, P. G. M.; Oehrlein, G. S.; Cook, J. M. *J. Vac. Sci. Technol.* **1999**, *A17*, 26.

(3) Endo, K.; Shinoda, K.; Tatsumi, T. *J. Appl. Phys.* **1999**, *86*, 2739.

(4) Shirafuji, T. *Oyo Butsuri* **1999**, *68*, 532 (in Japanese).

(5) Hiraoka, K.; Mizuno, T.; Eguchi, D.; Takao, K.; Iino, T.; Yamabe, S. *J. Chem. Phys.* **2002**, *116*, 7574.

(6) Hiraoka, K.; Takao, K.; Iino, T.; Nakagawa, F.; Suyama, H.; Mizuno, T.; Yamabe, S. *J. Phys. Chem. A* **2002**, *106*, 603.

(7) Hunter, E. L.; Lias, S. G. *J. Phys. Chem. Ref. Data* **1998**, *27*, 413.

(8) Kebarle, P. In *Techniques for the Study of Ion−Molecule Reactions*; Farrar, J. M., Saunders, W. H., Eds.; Wiley: New York, 1988.

(9) Hiraoka, K. *J. Chem. Phys.* **1987**, *87*, 4048.

(10) Becke, A. D. *J. Chem. Phys.* **1993**, *98*, 5648.

(11) Frisch, M. J.; Trucks, G. W.; Schlegel, H. B.; Scuseria, G. E.; Robb, M. A.; Cheeseman, J. R.; Zakrzewski, V. G.; Montgomery, J. A., Jr.; Stratmann, R. E.; Burant, J. C.; Dapprich, S.; Millam, J. M.; Daniels, A. D.; Kudin, K. N.; Strain, M. C.; Farkas, O.; Tomasi, J.; Barone, V.; Cossi, M.; Cammi, R.; Mennucci, B.; Pomelli, C.; Adamo, C.; Clifford, S.; Ochterski, J.; Petersson, G. A.; Ayala, P. Y.; Cui, Q.; Morokuma, K.; Malick, D. K.; Rabuck, A. D.; Raghavachari, K.; Foresman, J. B.; Cioslowski, J.; Ortiz, J. V.; Stefanov, B. B.; Liu, G.; Liashenko, A.; Piskorz, P.; Komaromi, I.; Gomperts, R.; Martin, R. L.; Fox, D. J.; Keith, T.; Al-Laham, M. A.; Peng, C. Y.; Nanayakkara, A.; Gonzalez, C.; Challacombe, M.; Gill, P. M. W.; Johnson, B. G.; Chen, W.; Wong, M. W.; Andres, J. L.; Head-Gordon, M.; Replogle, E. S.; Pople, J. A. *Gaussian 98*, revision A.7; Gaussian, Inc.: Pittsburgh, PA, 1998.

(12) Pai, R. Y.; Christophorou, L.G.; Christodoulides, A. A. *J. Chem. Phys.* **1979**, *70*, 1169.

(13) Hierl, P. M.; Paulson, J. F. *J. Chem. Phys.* **1984**, *80*, 4890.